REMOTE SENSING OF ATMOSPHERIC GASES BY AN IR LASER SPECTROMETER IN THE 3-μm RANGE AT A RESOLUTION OF 0.1 cm⁻¹

V.V. Krasnikov, M.S. Pshenichnikov, T.B. Razumikhina, V.S. Solomatin, and A.I. Kholodnykh

M.V. Lomonosov Moscow State University
Received October 23, 1989

Parameters and certain design features of an IR laser spectrometer (3-μm operating range) are described. It uses a differential frequency generator mixing the Nd: YAG laser radiation in a nonlinear crystal. Some results of remote sensing of atmospheric gases with the help of this spectrometer are discussed.

One of the principal problems faced by designers of a universal laser atmospheric gas analyzer is to extend its spectral sounding range into the domain where most of the atmospheric gas components absorb radiation, i. e., from 1.5 to 4.5 μm.

From this point of view semiconductor lasers, which feature a wide tuning frequency range in the IR (3–34 μm) and high spatial resolution (about 10^{-3}cm⁻¹), are of particular interest. Using these lasers for radiation sources, authors have measured the concentrations of such atmospheric gas constituents as CO (Ref. 1), NO, C_2H_4, H_2O (Ref. 2). However, semiconductor lasers are instruments of low output power, which means they can be used only along fairly short measurement paths (shorter than 300 m).

In Refs. 3 and 4 gas analyzers based on He-Ne lasers were employed to detect atmospheric methane and nitrogen oxide (at sensing wavelengths of 3.39 and 5.4 μm, respectively). The common drawback of these radiation sources is their fixed emission wavelength, so that only certain given atmospheric components can be sensed with their use.

We think that the more promising approaches Include parametric light generators with nonlinear frequency tuning,[5,6] and generators of summed[7] and difference[8] frequencies.

THE OPTICAL PART OF THE SPECTROMETER

The IR spectrometer presented in this paper employs the principle of successive frequency transformation from a standard YAG laser in nonlinear optical crystals and in tuned dye lasers. The source of tuned IR radiation is a difference frequency $\omega_e = \omega_1 - \omega_2$ generator with a KDP-crystal (here ω_1 and ω_2 are the YAG laser second harmonic and the tuned dye laser frequencies, respectively). The block diagram of the spectrometer emitter is given in Fig. 1. Multiple transformation of the standard YAG laser frequency is subject to strict limitations on its stability. That is why we employ a passive Q modu-

lation by a LiF crystal (F_2 dye centers) combined with a spectrally selective resonator cavity. We consider this method to obtain tuned narrow-band relatively powerful IR radiation to be acceptably simple and effective. The emitter was constructed on a rigid Duralumin plate, and had overall dimensions of 1000×500×200 mm and a mass of less than 40 kg.

New nonlinear − optical KDP-crystals were used for frequency doubling devices. Wide nonlinear receptivity, high radiation strength, and low temperature dependence of the synchronism angle make them advantageous compared with the frequency doubling devices usually employed. The latter circumstance is particularly important for field operations.

The tuned dye laser was built according to the well-known and recommended geometry of a grazing-incidence diffraction grating. which significantly increases its spectral resolution. Such a design makes possible a short resonator cavity (approximately 20 cm), permitting. in principle, single-mode generation. Two diffraction gratings were used as dispersive elements in the dye laser. The first (1800 lines/mm) operated in an almost grazing mode, within the first diffraction order, and the second (600 lines/mm) − in the autocollimation mode, also within the first diffraction order. Continuous frequency tuning was achieved by rotating the second grating by a stepping motor. Frequency tuning fineness amounted to 0.02 cm⁻¹ per step. Radiation left the cavity via the zero diffraction order.

Initially the TDL (tuned dye laser) wavelength was set by a silver limit switch. The change in wavelength was determined from the number of motor steps taken. Moreover, part of the radiation from the TDL was channeled to a Fabry-Perot etalon (free dispersion range of 0.67 cm⁻¹) for additional optical control. The absolute frequency calibration of the spectrometer was performed by comparing experimental spectra to computed, with its accuracy being ≈ 0.1 cm⁻¹.

The difference frequency was generated in the KDP-crystal during nonlinear mixing of the TDL radiation with the second harmonic of the YAG laser. A collinear interaction scheme was used. To

increase mixing efficiency both beams were independently focused into the nonlinear crystal and matched at a dichroic mirror. The IR radiation energy amounted to about 0.1 μJ. Preliminary experiments demonstrated that an additional amplifier for the YAG laser and a $LiNbO_3$ crystal as a difference frequency generator might raise this energy to 0.5—1.0 mJ.
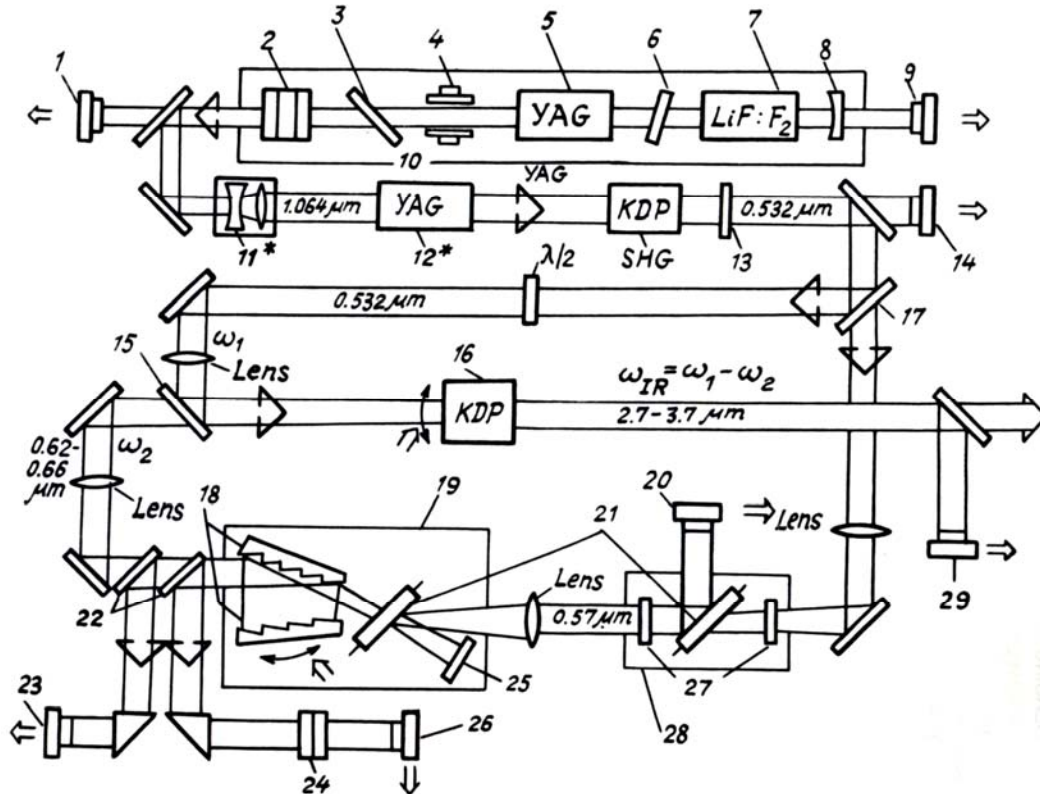
FIG. 1. Optical scheme of the IR laser spectrometer: elements connected to the computer (⇒), nonmandatory elements (*).
1) YAG energy control; 2) Stuck; 3) Brewster; 4) Diaphragm; 5) Active element; 6) Etalon; 7) Passive shutter; 8) Blind mirror; 9) Gate; 10) Reference; 11) Telescope*; 12) Amplifier*; 13) Filter; 14) SHG (second harmonic generator) control; 15) Dichroic mirror; 16) Difference frequency generator; 17) Splitting mirror; 18) Diffraction grating; 19) Narrow-band TDL; 20) TDL energy control; 21) Cell with dye; 22) Splitter plate; 23) TDL energy control; 24) Fabry-Perot etalon; 25) Blind mirror; 26) TDL frequency control; 27) Cavity mirror; 28) Intermediate TDL; 29) Measurement of output IR energy.

Depending on the type of dye used, the TDL generated in the following ranges: 632—660 nm (rhezosurine in ethanol) or 655—695 nm (carbarine-720 in ethanol with KOH added). At the center of the generation band the output radiation power amounted to 5 kW, its energy instability was less than 10%, and the line width amounted to 0.1 cm^{-1}. In that case the tuning range for the difference frequency amounted to 2.4—3.4 μm and could be easily extended to 4.5 μm (the transparency limit for the KDP-crystal), if one used phenalemine-160 for the laser dye.

The difference frequency was continuously tuned by the synchronous rotation of the TDL diffraction grating and the KDP-crystal.

SPECTROMETER AUTOMATION SYSTEM

The task of designing a laser IR spectrometer had the goal of producing a durable instrument fit to be operated by users poorly acquainted with laser technology. Obviously, to reach this goal it is necessary to completely automate both the measurement procedure and the functional control of the various spectrometer units. Demands for small size, low cost, and simultaneous high durability forced us to reject DVK computer complexes and CAMAC-type interface systems (although widely used, they have become neither cheaper nor more available). We have chosen a household computer, the BK-0010. Its price is lower than that of practically any CAMAC module, and the capacities are similar to those of the DVK processor. A relatively small memory capacity and lack of a DOS are not critical for our task. At the same time its adequately dynamic graphics with good resolution makes it possible to display the data on a real-time basis.

A block diagram combining the principal units of the spectrometer automation system is shown in Fig. 2.
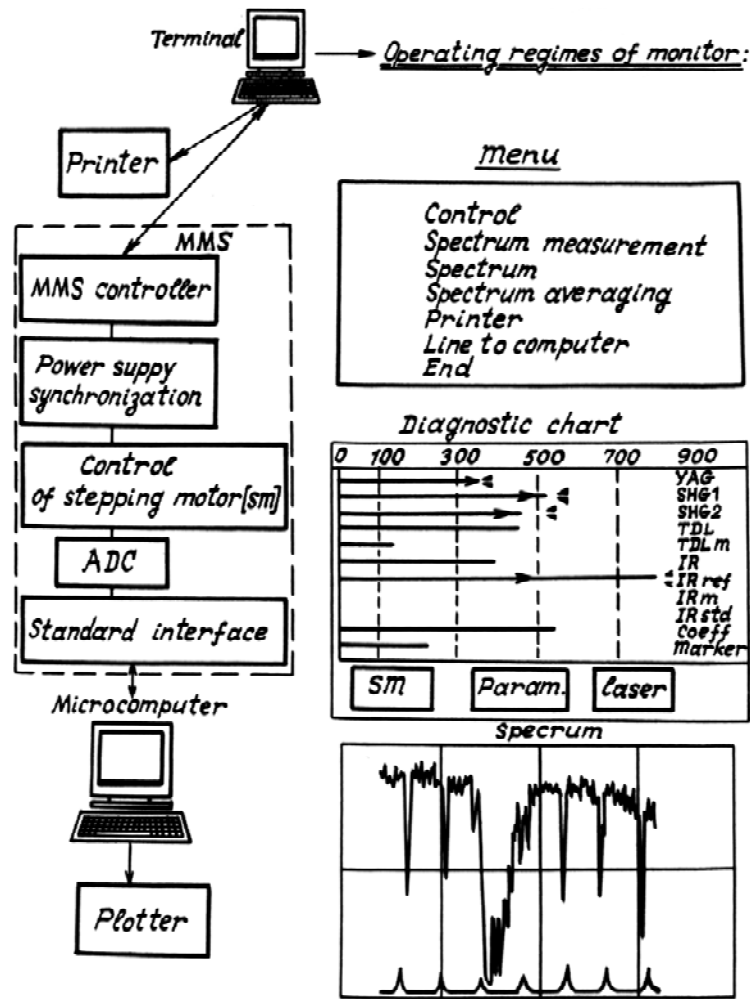
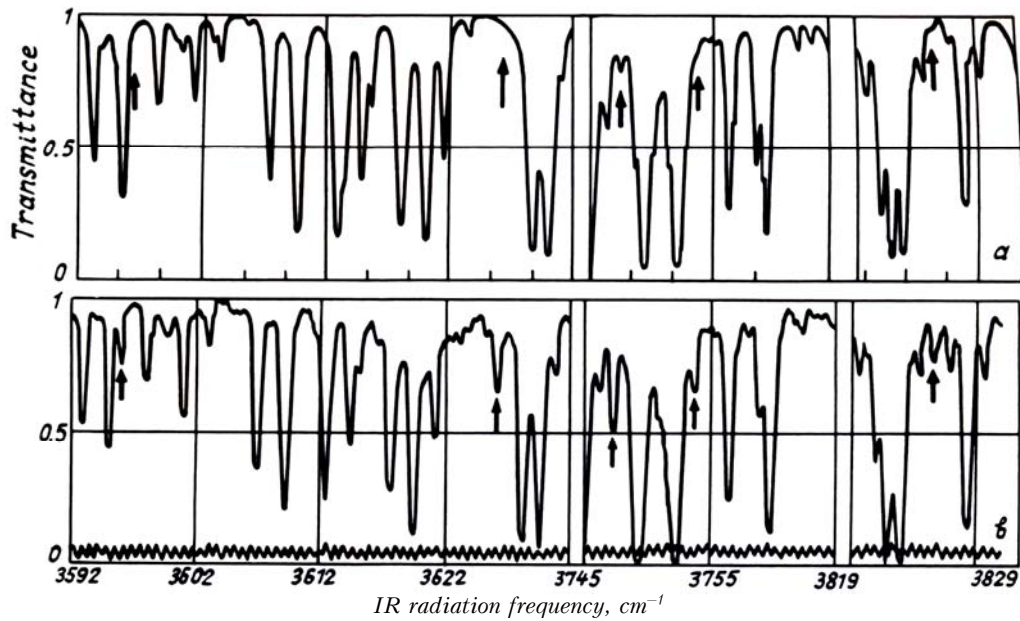FIG. 2. Block diagram, of the automatic system and practical operating modes of the controlling monitor.

FIG. 3. Fragments of water vapor absorption spectra. Calculations in accordance with Ref. 11: sensing radiation half-width — 0.1 cm^{-1}, number of absorbing molecules along the beam path — $1.8 \cdot 10^{19}$ cm^{-2}(a); experiment: 25-cm cell, water vapor concentration — $8 \cdot 10^{17}$ cm^{-3}(b). Arrows indicate water vapor absorption lines, the intensity of which differed drastically from computed value.

Spectrometer elements are interfaced with the computer via a specially designed modular main system (MMS), which work well with the BK-0010 in terms of its size and price. The MMS channel is suitable for modern LIS, ADC, DAC, PLM, and also for a microprocessor complex of the K-580 series, (see Ref. 10), and has a simple exchange protocol. Such organization of the system has resulted in modules only 110x160x15 mm in size, with their interface parts containing one or two, and their functional parts from two to ten microchips.

The MMS system is built as a separate crate $460 \times 230 \times 150$ mm in size, holding up to eight modules; Its mass is less than 8 kg.

As for the spectrometer software, the following functions were delegated to it: 1) dialogue interaction with the operator; 2) control of IR frequency scanning; 3) continuous control of frequency change; 4) statistical data processing and its storage in a user-friendly format; 5) rapid monitoring of functional state of the spectrometer elements; 6) exchange of needed information with a central computer within a local computer network. The software, formatted in the DVK computer, employs PASCAL and MACRO-11 languages. The BK is loaded either from magnetic tape (a household tape-recorder can be used) or via a local network.

The TDL frequency is initially set during spectrometer switch-on. Simultaneously, the KDP crystal synchronism angle is adjusted and the parameters of the laser radiation are checked. To measure transmission spectra it is enough to set the frequency tuning range, the scanning step and the number of averaging pulses. So the data accumulate, the resulting spectrum is displayed on a monitor (a domestic TV set is used). At any moment the operator can switch into the test-mode. In this mode amplitude scales (ADC units) can be displayed together with the energy of light pulses in ADC units and certain other information (see Fig. 2). Routine operation of this test-indicator demonstrated its extreme usefulness for adjusting various optical units and quick checking of the entire system.

Upon completion of the measurements and primary processing, the spectral dependences are kept as hardcopies of the screen (printouts or tapes). If spectra need be filed or identified using spectroscopic data banks, the data from the BK computer can be transmitted to a master computer via a local computer network. Availability of a standard asynchronous interface makes possible operation of the spectrometer from a remote terminal or via the master computer.

MEASUREMENT RESULTS

The described instrument can be used first as a lab IR spectrometer, and second — as a field path gas analyzer. We performed experiments in both of these modes. Transmission spectra of the following gases were taken: N_2O — the $\nu_1 + \nu_3$ band centered at 3500 cm^{-1}; CO_2 — the $2\nu_2 + \nu_3$ and $\nu_1 + \nu_3$ bands centered at 3609 and 3716 cm^{-1}, respectively; CH_4 — the ν_3 band centered at 3020 cm^{-1}; H_2O — the $2\nu_2$, ν_1, and ν_3 bands, centered at 3190, 3650, and 3755 cm^{-1}, respectively. An 80-cm long cell at a test gas pressure of about 5 Torr and a total cell pressure of 1 atm was employed. According to available estimates, self-broadening of absorption lines at such pressures is significantly lower that broadening by buffer gas (nitrogen in our case). Therefore, such cell measurements can be assumed to simulate field path sensing of the atmosphere.

For IR radiation sensors we used PbS (FSB-16AN) and PbSe (SF-4) uncooled photoreceivers (PR).

Experimental vs. computed spectral comparisons yielded absolute frequency calibration of the spectrometer and an assessment of its spectral resolution, which amounted to approximately 0.15 cm^{-1}.

Figure 3 presents fragments of water vapor transmission spectra between 3600 and 3800 cm^{-1}. A 25-cm cell contained $8 \cdot 10^{17}$ cm^{-3} of water vapor (it is equal to 100% humidity at 25°C and 1 atm of total pressure). The same figure shows a spectrum computed from atlas data[11] following the routine described in Ref. 6. During calculations the line half-width was taken at 0.1 cm^{-1}. Both spectra agree well, although certain discrepancies are also present. For example, the water vapor transmission measured lower at 3747.39 and 3753.81 cm^{-1} in all the experimental series, as if the actual line intensities at these frequencies were an order of magnitude above the atlas values.

In addition, as seen from Fig. 3, there are certain lines in the absorption spectra absent in the atlas[11] (at least within the experimental frequency reference), e.g., at $\nu = 3596.13$, 3626.18, 3824.24 cm^{-1}. According to available estimates absorption cross sections for these lines were about $1.5 \cdot 10^{-20}$, $5 \cdot 10^{-20}$, and $1 \cdot 10^{-20}$ cm^2, respectively. The accuracy of the frequency determination is about 0.1 cm^{-1}, and is certified by a relative frequency calibration. This calibration was done using a Fabry-Perot interferometer with a 0.675 cm^{-1} free dispersion range (see frequency markers below the presented spectra).

For systematic path measurements of atmospheric transmission a flat aluminum mirror of 80-cm diameter was mounted at the end the path. Reflected radiation, focused by a BaF_2 lens (12-cm diameter, 50-cm focal length), fell upon an InSb photodiode, cooled by liquid nitrogen, having a sensitivity of 10^9 cm $\cdot$ W^{-1} $\cdot$ Hz$^{-1/2}$. The photodiode was mounted close to the spectrometer itself. To amplify the signal from the photoreceiver (PR), the spectrometer output radiation was collimated by a 20-cm focal length BaF_2 lens. For a path length of 120 m the PR signal-to-noise ratio in the atmospheric transmission maximum amounted to at least 30.
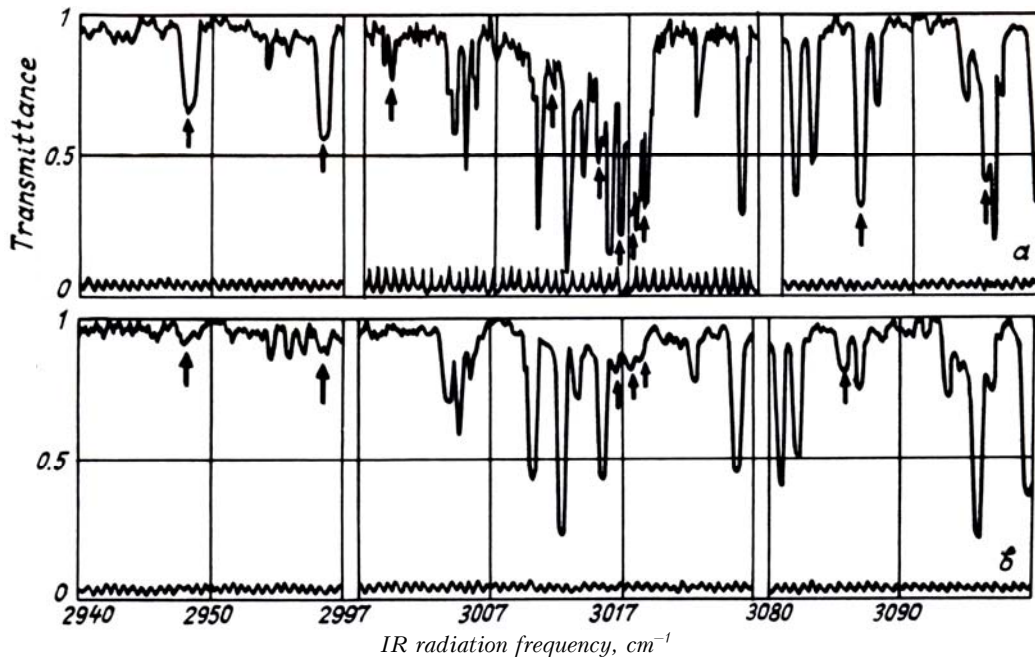
FIG. 4. Fragments of the atmospheric absorption spectra along a beam path of 55 m: 5-cm cell introduced into the beam path, methane concentration of 10^3 ppm (a); "clean" path (b). Arrows indicate positions of the CH_4 absorption lines.

Fragments of the atmospheric transmission spectrum (55-m path) are displayed in Fig. 4b. Experiments were staged on the premises of the Moscow State University Department of Nonlinear Optics from May to June 1989. Apart from water vapor, the spectra obtained clearly show methane absorption lines. For more reliable identification of the latter an additional 5-cm cell was introduced into the beam path. It contained 8 Torr of CH_4 plus 1 atm of air, bringing methane concentration in the cell to 10 ppm, see Fig. 4a. The spectra obtained from the 55-m path demonstrate reliable identification of CH_4 in its Q-band and the R(6) line. At longer paths (≥ 1 km) the P(5) and P(6) lines ($\lambda = 3.39$ μm) are better to use: water vapor lines there are significantly weaker than in the methane R-band. Computed vs. experimental spectra comparisons yield estimated average CH_4 concentration along the path at about 1–2 ppm. Path vs. cell measurements produce 1.5 ± 0.5 ppm of CH_4.

CONCLUSIONS

1. Lowering the spectral resolution limitations to 0.1 cm^{-1} makes it possible to construct a fairly simple spectrometer convenient in operation and handling, with its sensitivity loss at extremely low gas concentrations being rather insignificant (by a factor of two if both emission and absorption line widths remain identical).[12]

2. Water vapor spectra measurements indicate the resolution of 0.1 cm^{-1} to be sufficient to retrieve intensities of separate vibrational-rotational components. Certain H_2O absorption lines were found, the intensities of which differed significantly from their respective computed values. The locations of several microwindows, fit for diagnosing the presence of minor atmospheric gas components against the background of water vapor absorption, were identified.

3. Using the described spectrometer in combination with a mirror reflector, the background CH_4 can be identified from path lengths of about 50 m at signal-to-noise ratios of at least 10. The variety of available frequency ranges increases the accuracy of CH_4 determinations and also simplifies diagnostics of CH_4 against the heavy background of other pollutants with partially overlapping absorption lines.

REFERENCES

1. Yu.V. Kosichkin and A.I. Nadezhdenskii, Izv. Akad. Nauk SSSR, Ser. Fiz. **47**, No. 10, 2037 (1983).
2. E.D. Hinkley, Opt. Quantum Electron. **8**, 155 (1976).
3. Yu.A. Butikov, V.E. Kositsyn, and V.A. Tabarin, *Laser Absorption Techniques for Gas Microconcentration Analysis* (Energoatomizdat, Moscow, 1984).
4. S.A. Boiko, A.N. Bondar', A.I. Popov, and Yu.G. Putilov, Opt. Atm. **1**, No. 3. 116 (1988).
5. R.A. Baumgartner and R.L. Byer, Appl. Opt. **17**, No. 22, 3555 (1978).
6. V.I. Kuznetsov, A.V. Migulin, V.I. Pryalkin, T.B. Razumikhina, and A.I. Kholodnykh, Zh. Prikl. Spektrosk. **45**, No. 3. 468 (1986).
7. Yu.M. Andreev, S.N. Bovdei, P.P. Ceiko, A.I. Gribenyukov, V.A. Gurashvili, V.V. Zuev, and S.V. Izyumov, Opt. Atm. **1**, No. 4, 124 (1988).
8. V.V. Krasnikov, M.S. Pshenichnikov, T.B. Razumikhina, V.S. Solomatin, and A.I. Kholodnykh, *Abstract of Reports at the Thirteen Internal. Conf. Coll. and Nonlin. Opt*. Part 2, 225 (1988).

402 Atmos. Oceanic Opt. /April 1990/ Vol. 3, No. 4

V.V. Krasnikov et al.

9. M.G. Littman, Opt. Lett. No. 3, 138 (1978).
10. A.A. Myachev and V.V. Ivanov, *Computer System Interfaces Employing Mini- and Micro-computers* (Radio i Svyaz', Moscow, 1987).

11. A. Chedin, N. Husson, N. Scott, et al., The GEISA data bank 1984 version. Laboratoire de Meteorologie Dynamique du C.N.R.S., (1986).
12. A.V. Migulin and T.B. Razumikhina, Zh. Prikl. Spektrosk. **50**, No. 4, 604 (1989).